Supporting Information for:

Total Structural Determination of Alloyed Au15.37Cu16.63(S-Adm)20 Nanocluster with Double Superatomic Chains

Li Tang, [a, b] Shiyao Deng, [c] Shuxin Wang, [b, *] Yong Pei, [c, *] Manzhou Zhu [a, *]

[a]*Department of Chemistry and Centre for Atomic Engineering of Advanced Materials, AnHui Province, Key Laboratory of Chemistry for Inorganic/Organic Hybrid Functionalized Materials, Anhui University, Hefei, Anhui, 230601, P. R. China. E-mail: zmz@adu.edu.cn*

[b]*College of Materials Science and Engineering, Qingdao University of Science and Technology, Qingdao 266042, P. R. China. E-mail: shuxin_wang@qust.edu.cn*

[c]*Department of Chemistry, Key Laboratory of Environmentally Friendly Chemistry and Applications of Ministry of Education, Xiangtan University, Hunan Province, China, 411105, P.R. China. E-mail: ypei2@xtu.edu.cn*

Table of Contents

1. Experimental section

Materials

Tetrachloroauric(III) acid ($HAuCl_4 \cdot 3H_2O$, >99.99% metals basis, Aldrich), copper chloride ($CuCl_2 \cdot 2H2O$, >99.99% metals basis, Aldrich), 1-adamantanethiolate (HS-Adm, 98%), sodium borohydride ($NaBH_4$, Aldrich). Dichloromethane (HPLC grade, ≥99.5%, Aldrich), methanol (HPLC grade, ≥99.9%), ethanol (HPLC grade, ≥99.9%), ether (HPLC grade, ≥99.9%), pure water purchased from Wahaha Co. Ltd.

Note: All chemicals were used without further purification. All glassware was thoroughly cleaned with aquaregia (HCl/HNO_3 =3:1 vol%), rinsed with copious pure water, and then dried in an oven prior to use.

Synthesis of $Au_{15.37}Cu_{16.63}(S\text{-}Adm)_{20}$ NCs

For the nanocluster synthesis, $HAuCl_4 \cdot 3H_2O$ (0.075 mmol, 30 mg) was dissolved in 1mL H_2O and $CuCl_2$ (10 mg, 0.074 mmol) was dissolved in CH_3OH (3mL) and CH_2Cl_2(15 mL) with sonication. The solution was vigorously stirred (ca. 1500 rpm) with magnetic stirring for 20 min. Then, HS-Adm (200 mg, 1.2 mmol) was added and vigorously stirred (ca. 1500 rpm) for another 15 min. The CH_2Cl_2 phase changed from orange to light yellow and finally to colorless within 15 min. $NaBH_4$ (2.64 mmol, 100 mg) dissolved in 5 mL ice-cold pure water was quickly added to the solution; the colorless solution turned dark immediately. The reaction was continued for 12 h under a N_2 atmosphere. After that, the aqueous layer was removed, the mixture in the organic phase was dried by using a rotary evaporator, more methanol was added to wash away excess ligand, and precipitate was extracted by using CH_2Cl_2. This process was repeated many times. The yield of $Au_{15.37}Cu_{16.63}(S\text{-}Adm)_{20}$ is >70% (Au atom basis). The as-prepared nanocluster was crystallized in $CH_2Cl_2/C_4H_{10}O$ at room temperature.

Rod-like single crystals were crystallized in CH_2Cl_2/ $C_4H_{10}O$ at room temperature over 3-4 days. (Figure S10).

2. Characterization

All UV-Vis absorption spectra of nanoclusters were recorded using an Agilent 8453. Samples were dissolved in CH_2Cl_2 to make a dilute solution and then moved to a quartz dish, followed by spectral measurements.

X-ray photoelectron spectroscopy (XPS) measurements were performed on a Thermo ESCALAB 250, with a mono chromated AlKα (1486.8 eV) 150 W X-ray source, 0.5 mm circular spot size, a flood gun to counter charging effects, and analysis chamber base pressure lower than 1 x 10^{-9} mbar. Data were collected with FAT= 20 eV. The sample was directly infused into the chamber at 5 μL/min.

Nuclear magnetic resonance (NMR) analysis was performed on a Bruker Avance spectrometer operating at 400 MHz for ^{2}H-NMR. CD_2Cl_2 was used as the solvent to dissolve ~ 10 mg clusters synthesized by $NaBD_4$.

The $Au_{15.4}Cu_{16.6}(S\text{-}Adm)_{20}$ nanocluster crystal data collection for single crystal X-ray diffraction was carried out on Stoe Stadivari diffractometer at 170 K, using Cu-Kα radiation (λ= 1.54186 Å). With the aid of Olex2, the structure was solved with the ShelXT structure solution program using Intrinsic Phasing, and refined with the ShelXL refinement package using Least Squares minimization. Detailed data was provided in Table S3.

3. Theoretical method

The geometric optimization of clusters and the electronic structure calculations were performed based on the density functional theory (DFT), using the Gaussian 09 software package[S1] at the PBE0[S2]/LanL2DZ [S3-S5] (metal) and 6-31 G(d) (other) levels[S6-S8]. The ground state wave function, determined by the DFT calculation, was then used as an input file of Multiwfn software package[S9] to carry out the Adaptive Natural Density Partitioning (ADNDP) analysis.

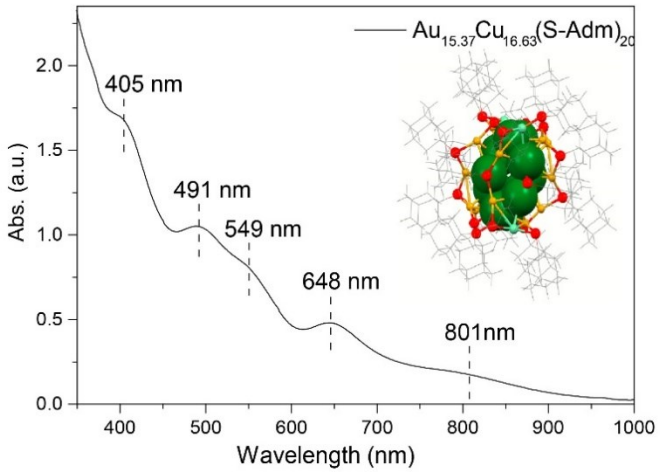

Figure S1 UV-vis absorption spectrum of $Au_{15.37}Cu_{16.63}(S\text{-}Adm)_{20}$ nanocluster in CH_2Cl_2, inset, along with the structure obtained by X-ray crystallography. Colours in the atomistic structures: green, Au; orange, Cu; red, S; turquoise, Au/Cu; gray, C/H.

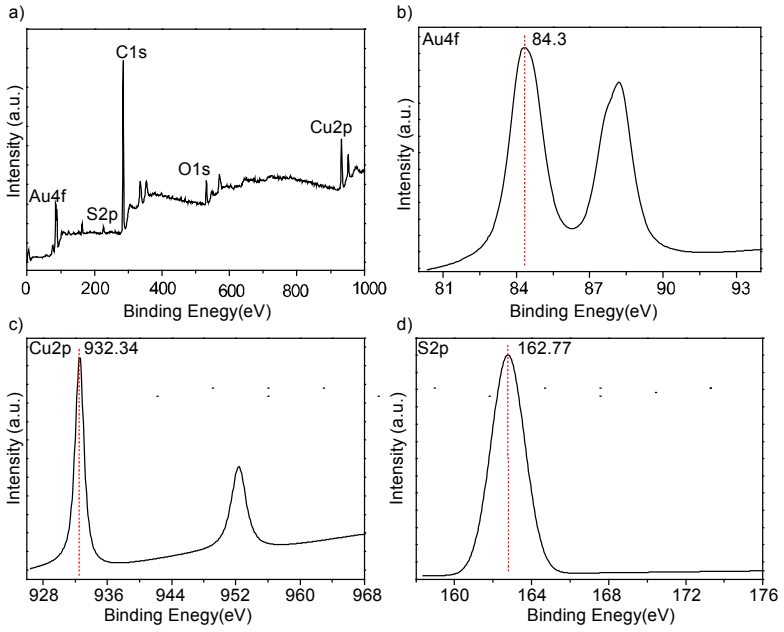

Figure S2 X-ray photoelectron spectroscopy (XPS) of $Au_{15.37}Cu_{16.63}(S\text{-}Adm)_{20}$ nanocluster. a) XPS, b) Au4f, c) Cu2p, d) S2p in $Au_{15.37}Cu_{16.63}(S\text{-}Adm)_{20}$ nanocluster.

Table S1 The atomic ratio of Au, Cu and S in $Au_{15.37}Cu_{16.63}(S\text{-}Adm)_{20}$ NCs calculated from X-ray photoelectric spectroscopy (XPS) measurements.

Measurement	Au (%)	Au (%)	S(%)
XPS results	29.41	31.38	39.21
crystal analysis results	15.5	16.6	20

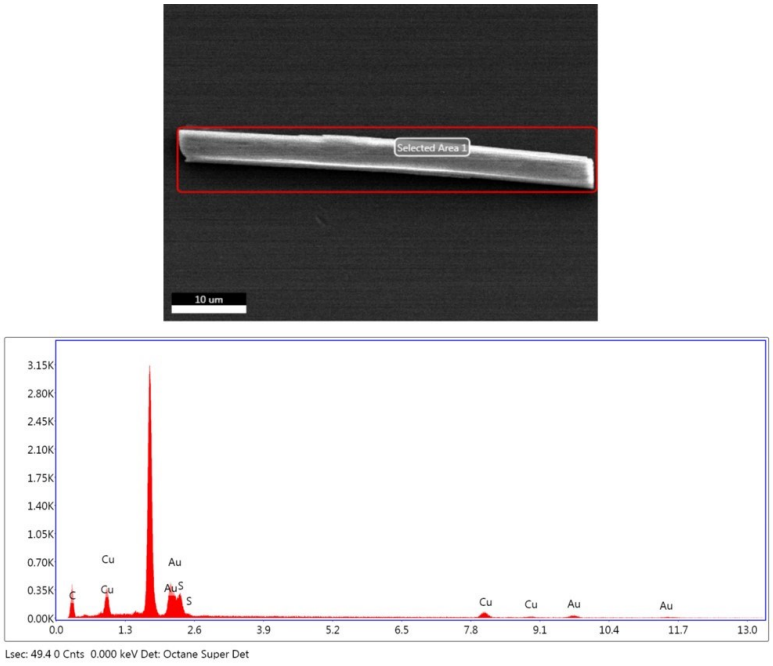

Figure S3 SEM image and energy-dispersive X-ray spectrum (EDX) of $Au_{15.37}Cu_{16.63}(SR)_{20}$.

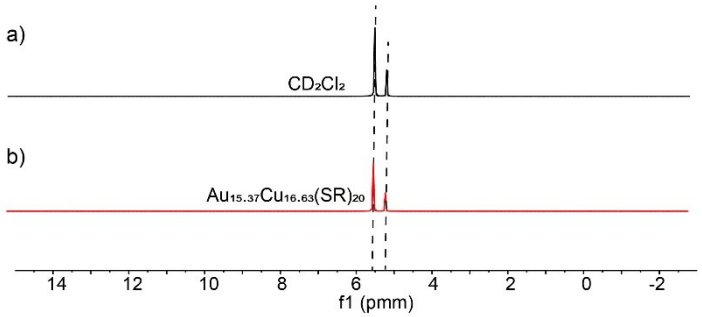

Figure S4 ^{2}H-NMR spectrum a) CD_2Cl_2 b) $Au_{15.37}Cu_{16.63}(SR)_{20}$ nanocluster in CD_2Cl_2.

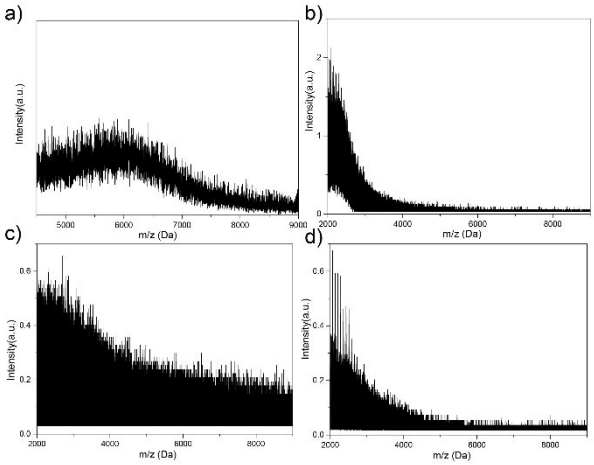

Figure S5. MS result of the $Au_{15.37}Cu_{16.63}(S\text{-}Adm)_{20}$ nanocluster. a) Positive-mode MALDI mass spectrum result; b) The ESI mass spectrum of the $Au_{15.37}Cu_{16.63}(S\text{-}Adm)_{20}$ nanocluster in positive mode by adding Cs+; c) The ESI mass spectrum of the $Au_{15.37}Cu_{16.63}(S\text{-}Adm)_{20}$ nanocluster in positive mode; d) The ESI mass spectrum of the $Au_{15.37}Cu_{16.63}(S\text{-}Adm)_{20}$ nanocluster in negative mode.

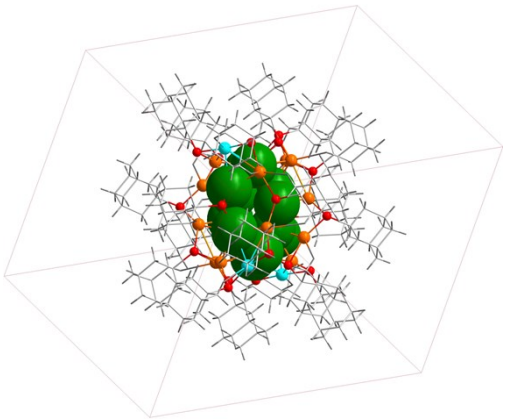

Figure S6 Unit cell comprising one $Au_{15.37}Cu_{16.63}(SR)_{20}$ nanocluster.

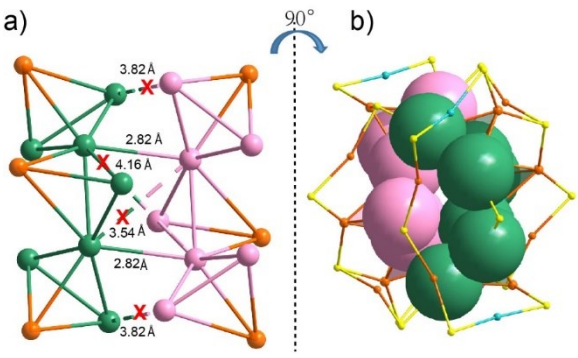

Figure S7 a) main view of Au-Au bond length of between two chains. b) side view of tunnel structure of $Au_{15.37}Cu_{16.63}(SR)_{20}$ nanocluster.

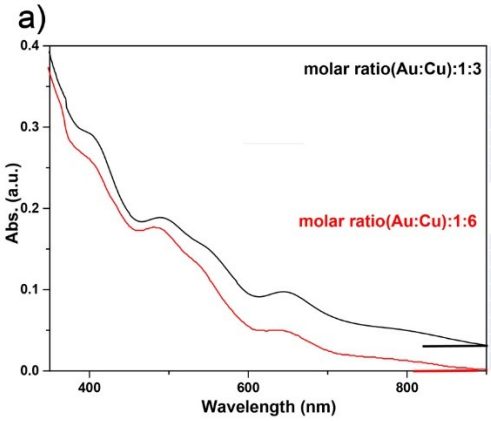

b)

Sites	Au%	Cu%	Total Au	Total Cu
1-2	35.10%	64.90%	0.702	1.298
3-4	33.70%	66.30%	0.674	1.326
5-12	0	100%	0	8
13-18	0	100%	0	6
19-32	100%	0	14	0
Total metal atoms			15.376	16.624
composition from the crystal structure			$Au_{15.376}Cu_{16.624}(SR)_{20}$	

c)

Sites	Au%	Cu%	Total Au	Total Cu
1-2	33.10%	66.90%	0.662	1.338
3-4	33.70%	66.30%	0.674	1.326
5-12	0	100%	0	8
13-18	0	100%	0	6
19-32	100%	0	14	0
Total metal atoms			15.336	16.664
composition from the crystal structure			$Au_{15.336}Cu_{16.664}(SR)_{20}$	

Figure S8 UV-vis spectrum and the metal occupancy information of **$(AuCu)_{32}$-II/III** in various molar ratio. a) UV-vis absorption spectrum of **$(AuCu)_{32}$-II** (black)and **$(AuCu)_{32}$-III** (red). The occupancy information of metal sites 1-32 in **$(AuCu)_{32}$-II** (b)and **$(AuCu)_{32}$-III** (c) nanoclusters.

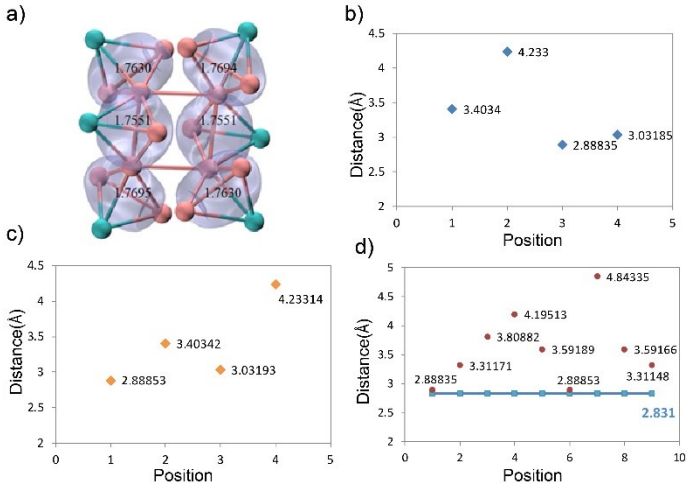

Figure S9 a) The density contour of six 4c-2e orbitals of the 12e $Au_{14}Cu_6^{8+}$ core according to the ADNDP analysis (Color code: pink= Au, cyan=Cu). Au-Au bond lengths distribution of tetrahedrons. b) The distance between Au atoms of tetrahedron 1,6. c) The distance between Au atoms of tetrahedron 3,4. d) The distance between Au atoms of tetrahedron 2,5.

Table S2 Distribution of bond lengths of Au-Au and Au-Cu bonds in tetrahedrons (Å).

Tetrahedron	Bond Type	Distance	Tetrahedron	Bond Type	Distance	Tetrahedron	Bond Type	Distance
1	Au-Au	2.748	2	Au-Au	2.762	3	Au-Au	2.702
	Au-Au	2.758		Au-Au	2.777		Au-Au	2.780
	Au-Au	2.864		Au-Au	2.831		Au-Au	2.929
	Au-Cu	2.649		Au-Cu	2.672		Au-Cu	2.641
	Au-Cu	2.687		Au-Cu	2.723		Au-Cu	2.796
	Au-Cu	2.780		Au-Cu	2.756		Au-Cu	2.841
4	Au-Au	2.748	5	Au-Au	2.762	6	Au-Au	2.702
	Au-Au	2.758		Au-Au	2.777		Au-Au	2.780
	Au-Au	2.864		Au-Au	2.831		Au-Au	2.929
	Au-Cu	2.649		Au-Cu	2.672		Au-Cu	2.641
	Au-Cu	2.687		Au-Cu	2.723		Au-Cu	2.796
	Au-Cu	2.780		Au-Cu	2.756		Au-Cu	2.841

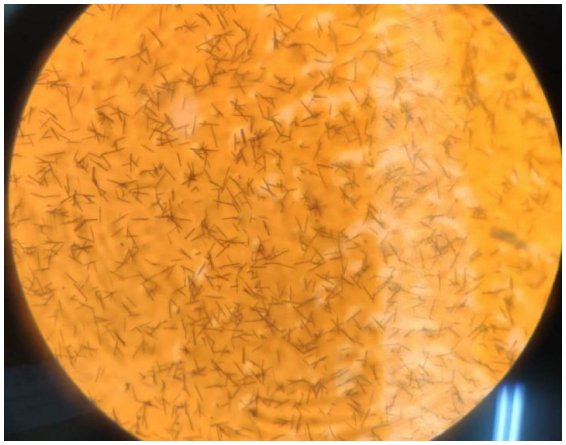

Figure S10 Photograph of $Au_{15.37}Cu_{16.63}(S\text{-}Adm)_{20}$ crystals.

Table S3 Crystal data and structure refinement for the $Au_{15.37}Cu_{16.63}(S\text{-}Adm)_{20}$.

Identification code	$Au_{15.37}Cu_{16.63}(S\text{-}Adm)_{20}$	
Empirical formula	$C_{200}H_{300}Au_{15.37}Cu_{16.63}S_{20}$	
Formula weight	7429.63	
Temperature/K	120	
Wavelength/Å	1.54186	
Crystal system	triclinic	
Space group	P-1	
Unit cell dimensions	a = 17.4596(9) Å	α= 103.748(4) °
	b = 18.8819(10) Å	β= 110.733(4) °
	c = 19.6255(10) Å	γ= 93.756(4)°
Volume/$Å^3$	5797.3(5)	
Z	1	
Density (calculated)/Mg/m^3	2.128	
Absorption coefficient/mm^{-1}	21.334	
F(000)	3516	
Theta range for data collection/°	2.972 to 67.500	
Index ranges	-20<=h<=18, -15<=k<=22, -23<=l<=19	
Reflections collected	49313	
Independent reflections	20077 [R(int) = 0.0985]	
Completeness to theta = 25.242°	96%	
Max. and min. transmission	0.9811 and 0.3484	
Data / restraints / parameters	1137/2710/20077	
Goodness-of-fit on F^2	0.997	
Final R indices [I>2sigma(I)]	R1 = 0.0856, wR2 = 0.2071	
R indices (all data)	R1 = 0.1261, wR2 = 0.2247	
Largest diff. peak and hole/ e $Å^{-3}$	5.965 and -5.120	

References

S1. Gaussian 09, Revision A.1, M. J. Frisch, G. W. Trucks, H. B. Schlegel, G. E. Scuseria, M. A. Robb, J. R. Cheeseman, G. Scalmani, V. Barone, B. Mennucci, G. A. Petersson, H. Nakatsuji, M. Caricato, X. Li, H. P. Hratchian, A. F. Izmaylov, J. Bloino, G. Zheng, J. L. Sonnenberg, M. Hada, M. Ehara, K. Toyota, R. Fukuda, J. Hasegawa, M. Ishida, T. Nakajima, Y. Honda, O. Kitao, H. Nakai, T. Vreven, J. A. Montgomery, Jr., J. E. Peralta, F. Ogliaro, M. Bearpark, J. J. Heyd, E. Brothers, K. N. Kudin, V. N. Staroverov, R. Kobayashi, J. Normand, K. Raghavachari, A. Rendell, J. C. Burant, S. S. Iyengar, J. Tomasi, M. Cossi, N. Rega, J. M. Millam, M. Klene, J. E. Knox, J. B. Cross, V. Bakken, C. Adamo, J. Jaramillo, R. Gomperts, R. E. Stratmann, O. Yazyev, A. J. Austin, R. Cammi, C. Pomelli, J. W. Ochterski, R. L. Martin, K. Morokuma, V. G. Zakrzewski, G. A. Voth, P. Salvador, J. J. Dannenberg, S. Dapprich, A. D. Daniels, O. Farkas, J. B. Foresman, J. V. Ortiz, J. Cioslowski, and D. J. Fox, Gaussian, Inc., Wallingford CT, 2009.

S2. Matthias Ernzerhof and G. E. Scuseria, *J. Chem. Phys.*, 1999, **110**, 5029.

S3. T. H. Dunning Jr. and P. J. Hay, Ed. H. F. Schaefer III, 1977,**3**,1-28.

S4. P. J. Hay and W. R. Wadt, *J. Chem. Phys.*, 1985, **82**, 270-83.

S5. W. R. Wadt and P. J. Hay, *J. Chem. Phys.*, 1985, **82**, 284-98.

S6. P. C. Hariharan and J. A. Pople, *Theor. Chem. Acc.*, 1973, **28**, 213-22.

S7. R. Ditchfield, W. J. Hehre, and J. A. Pople. *J. Chem. Phys.*, 1971, **54**, 724.

S8. G. A. Petersson, A. Bennett, T. G. Tensfeldt, M. A. AlLaham, W. A. Shirley, and J. Mantearis, *J. Chem. Phys.*, 1988, **89**, 2193-218.

S9. T. Lu, F. Chen, *Journal of Computational Chemistry*, 2012, **33**, 580–592.